Available online at www.sciencedirect.com
ScienceDirect
Icarus 189 (2007) 409–423
ICARUS
www.elsevier.com/locate/icarus

The radiolysis of SO_2 and H_2S in water ice: Implications for the icy jovian satellites

M.H. Moore [a,*], R.L. Hudson [b], R.W. Carlson [c]

[a] *Code 691, Astrochemistry Branch, NASA Goddard Space Flight Center, Greenbelt, MD 20771, USA*
[b] *Department of Chemistry, Eckerd College, St. Petersburg, FL 33733, USA*
[c] *Jet Propulsion Laboratory, California Institute of Technology, Pasadena, CA 91109, USA*

Received 6 June 2006; revised 4 January 2007

Available online 7 March 2007

Abstract

Spectra of Europa, Ganymede, and Callisto reveal surfaces dominated by frozen water, hydrated materials, and minor amounts of SO_2, CO_2, and H_2O_2. These icy moons undergo significant bombardment by jovian magnetospheric radiation (protons, electrons, and sulfur and oxygen ions) which alters their surface compositions. In order to understand radiation-induced changes on icy moons, we have measured the mid-infrared spectra of 0.8 MeV proton-irradiated SO_2, H_2S, and H_2O-ice mixtures containing either SO_2 or H_2S. Samples with H_2O/SO_2 or H_2O/H_2S ratios in the 3–30 range have been irradiated at 86, 110, and 132 K, and the radiation half-lives of SO_2 and H_2S have been determined. New radiation products include the H_2S_2 molecule and HSO_3^-, HSO_4^-, and SO_4^{2-} ions, all with spectral features that make them candidates for future laboratory work and, perhaps, astronomical observations. Spectra of both unirradiated and irradiated ices have been recorded as a function of temperature, to examine thermal stability and phase changes. The formation of hydrated sulfuric acid in irradiated ice mixtures has been observed, along with the thermal evolution of hydrates to form pure sulfuric acid. These laboratory studies provide fundamental information on likely processes affecting the outer icy shells of Europa, Ganymede, and Callisto.
Published by Elsevier Inc.

Keywords: Ices; Jupiter, satellites; Ices; IR Spectroscopy; Satellites, surfaces

1. Introduction

Spectra of Jupiter's icy satellites reveal surfaces with significant amounts of water ice (Calvin et al., 1995) with minor amounts of sulfur dioxide, SO_2 (Lane et al., 1981; Noll et al., 1995), carbon dioxide, CO_2 (Smythe et al., 1998), and hydrogen peroxide, H_2O_2 (Carlson et al., 1999a), along with hydrated materials (McCord et al., 1998b; Carlson et al., 2005, 1999b). Molecular oxygen (O_2) has been identified in Europa, Ganymede, and Callisto's surfaces (Spencer and Kleasman, 2001; Spencer and Calvin, 2002), and forms atmospheres on Europa and Ganymede (Hall et al., 1995, 1998). Ozone (O_3) has been found only on Ganymede (Noll et al., 1996). The reduced form of sulfur, hydrogen sulfide (H_2S), has not been unequivocally identified, but it is a candidate for the 3.88-μm feature detected on Ganymede and Callisto (McCord et al., 1998a). Elemental sulfur has been suggested as a component of Europa's dark material (McEwen, 1986; Johnson et al., 1988; Spencer et al., 1995; Carlson et al., 1999b).

These spectral identifications are "snapshots" of dynamic surfaces that undergo chemical modification by interactions with the jovian magnetosphere on relatively short timescales. On Europa, the ∼100 μm ice thickness sampled by near-infrared (near-IR) measurements receives a significant radiation dose of ∼1 eV per 16-amu molecule per year from all protons and electrons (Cooper et al., 2001). A similar dose in Ganymede's polar region takes about 30 years, whereas in the magnetically shielded equatorial region it requires nearly 400 years. On Callisto, about 700 years are need. These time estimates are derived from the dose vs depth curves of Cooper et al. (2001). Table 1 summarizes the radiation and temper-

* Corresponding author. Fax: +1 301 286 0440.
E-mail address: marla.h.moore@nasa.gov (M.H. Moore).

0019-1035/$ – see front matter Published by Elsevier Inc.
doi:10.1016/j.icarus.2007.01.018

Table 1
Temperature and radiation environments on jovian icy satellites

Satellite	Materials suggested	Temperature (K)	Global average energy from ion and e^- flux (keV cm^{-2} s^{-1})[a]	Average number flux (cm^{-2} s^{-1}) and energy[a]	Time to accumulate 1 eV per molecule in top 100 μm (yr)[a]
Europa	H_2O, SO_2, CO_2, H_2O_2, O_2, H_2SO_4, carbonate salts, hydrous sulfate	86–132[b]	8×10^{10}	(H^+) 1.5×10^7 800 keV (e^-) 1.8×10^8 340 keV	1
Ganymede	H_2O, SO_2, SH, CO_2, CH, XCN, H_2O_2, O_2, O_3, hydrated and hydroxylated minerals	~124[c]	5×10^9 (poles)	(H^+) 3.8×10^6 263 keV (e^-) 3.1×10^7 100 keV	6
			3×10^8 (equator)	(H^+) 5.9×10^3 5.4 MeV	80
Callisto	H_2O, SO_2, SH, CO_2, CH, XCN, H_2O_2, hydrated and hydroxylated minerals	~115[c]	2×10^8	(H^+) 1.6×10^5 143 keV (e^-) 1.8×10^6 66 keV	140

[a] Depth profiles for total volume dosage rate are from Cooper et al. (2001, Fig. 16).
[b] Spencer et al. (1999).
[c] Disk-averaged temperatures of sublimating H_2O-ice from Grundy et al. (1999).

ature environments, and known chemical components, of the icy Galilean satellites. With the exception of the equatorial region of Ganymede, high-energy protons and electrons are the dominant contributors of ionizing energy. However, compared to Ganymede or Callisto, Europa has the largest global energy flux of electrons and protons and receives the largest dose per volume at any depth (Cooper et al., 2001).

The sources of sulfur species on Jupiter's icy satellites may be connected to implanted Iogenic sulfur ions and micrometeoroid impacts, but it is difficult to separate these exogenic sources from the radiation processing of endogenous sulfur species. In particular, Europa may provide emplacement of sulfur-bearing compounds from a possible brine or acid subsurface ocean (Marion, 2002; Kargel et al., 2000, 2001). The source of carbon species may be connected to exogenic carbonaceous material from comets and micrometeorite impacts (Pierazzo and Chyba, 2002). The source of H_2O_2, O_2, and O_3 is radiation processing of the surface ice, and these three molecules are evidence that radiation products form at abundances sufficient for detection (Johnson et al., 2003). In all cases, it is thought that radiolysis and photolysis products undergo downward mixing by meteoritic gardening, sublimation, burial, and subduction, suggesting that they can be transported to and trapped within regions much greater than their formation depth.

Although terrains showing symmetric, H_2O-ice-like IR bands are found on Europa, geological regions dominated by distorted H_2O-ice bands are ubiquitous, as observed with Galileo's near-IR mapping spectrometer (NIMS). One suggestion to explain the spectral data is that they are consistent with the presence of hydrated sulfuric acid, $H_2SO_4 \cdot nH_2O$ where $n = 1$, 2, 3, 4, 6.5, or 8, produced on Europa's surface by radiolysis (Carlson et al., 1999b, 2002, 2005). Each of these hydrates has both a unique mid-IR spectrum (Zhang et al., 1993) and a specific temperature and pressure region of stability, although multiple hydrates can coexist within an ice. Carlson et al. (1999b, 2002, 2005) noted that the presence of both H_2O and SO_2 in an icy surface exposed to an intense radiation field suggests that sulfuric acid is a likely radiation product. They pointed out that H_2SO_4 is a common component of the atmospheres of Earth and Venus, due to the photochemistry of H_2O and SO_2. Carlson et al. (2005, 1999b) also showed that laboratory IR spectra of frozen $H_2SO_4 \cdot nH_2O$, where $n = 6.5$ and 8, could explain a major component of the NIMS spectra of hydrated surface regions of Europa.

An alternative suggestion for the distorted spectral bands seen on Europa is the presence of hydrated salt minerals such as $MgSO_4 \cdot 7H_2O$ and $Na_2CO_3 \cdot 10H_2O$ (McCord et al., 1998b, 1999, 2001, 2002). In this interpretation, the source of the salts is thought to be Europa's putative ocean. In both the acid and salt models, the distorted IR bands are thought to occur when water molecules form hydration shells around ions.

A third interpretation of the distorted spectral bands has been proposed recently by Clark (2004), who attributed them to the presence of hydronium ions (H_3O^+), rather than waters of hydration. This interpretation requires production of H_3O^+, presumably by radiolysis.

Sorting out likely surface materials and understanding their properties in the low-temperature radiation environment of Jupiter's moons requires input from laboratory experiments. Since H_2O-ice was the first material observed on the icy satellites, it is not surprising that it has been the subject of numerous laboratory studies. For example, it has long been known that when H_2O vapor is condensed below ~130 K, an amorphous solid can form. On warming, this material converts irreversibly to a cubic crystalline phase (within minutes at 155 K), and rapidly sublimes near 170 K in a 10^{-7}-Torr vacuum system.

The radiation-induced chemistry of amorphous H_2O-ice also has been investigated. Ion irradiation of pure H_2O-ice has been shown to form hydrogen peroxide, H_2O_2 (Moore and Hudson, 2000; Gomis et al., 2004a, 2004b; Loeffler and Baragiola, 2005; Loeffler et al., 2006) by in situ IR spectral measurements. The formation efficiency increases with the mass of the bombarding ion, and the H_2O_2 yield is greater at lower temperatures. Direct evidence for O_2 formation comes from its detection when it is sputtered from irradiated H_2O-ice (e.g., Johnson et al., 2005), and indirect evidence for O_2 formation comes from the detection of O_3 in irradiated H_2O-ice (Teolis et al., 2006).

Of the other Galilean-satellite ices, SO_2 and H_2S have received attention by experimentalists, although much less so than H_2O-ice. The IR spectrum of amorphous SO_2 at 9 K has been published, along with evidence that UV photolysis of SO_2-ice produces SO_3 (Salama et al., 1990; Schriver-Mazzuoli et al., 2003b). Much less has been published on H_2S-ice chemistry. An IR spectrum of amorphous 9 K H_2S is available, showing minimal change on photolysis of the sample (Salama et al., 1990).

Even less is known about ion radiation-induced chemistry of SO_2 and H_2S ices at Galilean satellite temperatures. Proton irradiations of SO_2-ice have been reported only for 20 and 88 K (Moore, 1984), with SO_3 being detected. The 0.25–1.25 μm transmission spectra of keV ion-irradiated SO_2 films showed increased absorption in the 0.3–0.8 μm region, consistent with the formation of short-chain sulfur species (Strazzulla et al., 1993), and similar results were obtained by O'Shaughnessy et al. (1988) who bombarded H_2O-ice with SO_2^+ ions.

In light of the scarcity of laboratory data on sulfur-containing ices at temperatures relevant to the Galilean satellites, we have performed a systematic set of experiments on irradiated H_2O-ice mixtures containing the molecules H_2S and SO_2. We present new results on the radiation destruction of SO_2 and H_2S in H_2O-ice, and the formation and stability of new species. Slow chemical or physical processes that might take years on the Galilean satellites were studied by heating irradiated ices.

2. Experimental methods

In our work we studied ices using the mid-IR spectral region, since it contains strong diagnostic IR absorptions of molecules, making it the prime region for identification of product species; the near-IR region contains weaker, and less characteristic, overtone absorption bands. The concentration ratios for ice mixtures examined were typically $H_2O/SO_2 = 3$ and 30, and $H_2O/H_2S \approx 10$. Proton irradiations of mixtures were done at 86, 110, and 132 K, values covering the equatorial temperatures observed on Europa (Spencer et al., 1999). Studies of single-component ices included lower temperature measurements.

Details of our experimental set-up, ice preparation, IR spectral measurements, cryostat, and proton beam source have been published (e.g., Hudson and Moore, 2004; Moore and Hudson, 2003). Briefly, gas mixtures were prepared in a vacuum manifold and then condensed onto a pre-cooled, gold-coated aluminum mirror inside a stainless-steel high-vacuum chamber ($\sim 10^{-7}$ Torr). The gold coating on the mirror minimized surface reactions that might have produced, for example, aluminum sulfate. Using two separate deposition lines, simultaneous controlled flows of H_2O vapor and either SO_2 or H_2S gas produced ice mixtures with $H_2O/SO_2 = 3$ and 30, and $H_2O/H_2S \approx 10$, depending on the experiment. The flow rate from each deposit tube was calibrated in separate experiments. Appropriate control experiments were done by warming unirradiated ice mixtures to check for possible thermally-induced reactions. In no case was a residual material formed in an unirradiated ice.

Gas mixtures were condensed and irradiated at 86 K, or condensed at 86 K and then warmed to 110 or 132 K before irradiation. The resulting ices were amorphous in phase. Samples could be maintained at any temperature from ~10 to 300 K depending on the ice composition. IR spectra with a range of 4000–400 cm^{-1} (2.5–25 μm) and a resolution of 4 cm^{-1} were taken by diverting the beam of the FTIR spectrometer (Mattson Polaris or Nicolet Nexus) toward the ice film. The beam passed through the ice before and after reflecting at the ice-mirror interface, and then went on to an IR detector. Most ice films examined were 3–5 μm thick, as determined by a laser interference fringe system.

Ices were processed by turning the sample mirror to face a beam of 0.8 MeV protons generated by a Van de Graaff accelerator. Radiation doses were determined by measuring the proton fluence ($p^+ cm^{-2}$) in the metal substrate beneath the ice sample and then converting to a common scale of eV per 16-amu molecule, referred to as simply eV $molec^{-1}$ or eV per molecule in the remainder of this paper. Stopping powers were calculated with Ziegler's SRIM program (Ziegler et al., 1985; www.srim.org) to be 289, 216, and 234 MeV $cm^2 g^{-1}$ for H_2O, SO_2, and H_2S, respectively. For mixtures we used the weighted average of the stopping powers for 0.8 MeV protons in H_2O and either SO_2 or H_2S, with the weighting factor based on the initial H_2O/SO_2 or H_2O/H_2S ratio in the ice mixture. A density of 1.00 g cm^{-3} was assumed for all samples containing H_2O.

Reagents used and their purities were as follows: H_2O (triply distilled, with a resistance greater than 10^7 Ohm cm), SO_2 (gas, Matheson, 99.98%), H_2S (gas, Matheson, 99.5%), CO_2 (gas, Matheson, 99.995%).

3. Results

Although our main interest was to understand the chemistry of irradiated $H_2O + SO_2$ ices, many background IR and irradiation experiments were needed involving single component ices SO_2 and H_2S and icy mixtures of $H_2O + H_2S$ and $H_2O + SO_2$. Since our experiments showed a progressive oxidation of sulfur following the sequence $H_2S \rightarrow SO_2 \rightarrow SO_4^{2-}$, we use this order to present the radiation experimental data. First, however, we discuss IR spectra of these unirradiated ices: (a) pure H_2S and SO_2, at temperatures from 10 to over 100 K, (b) $H_2O + H_2S$

mixtures from 86 to 110 K, and (c) $H_2O + SO_2$ mixtures from 86 to 110 K.

3.1. Unirradiated ices

3.1.1. IR spectra of H_2S and SO_2 ices

Fig. 1a shows IR spectra of pure H_2S deposited at 15 K and then warmed to 90 K. The 2555 cm^{-1} (ν_1) and 1172 cm^{-1} (ν_2) fundamental bands of H_2S are indicated (the weaker ν_3 fundamental near 2645 cm^{-1} is difficult to see and a $\nu_1 + \nu_2$ combination band at 3718 cm^{-1} is not shown). The structureless IR features at 15 K persisted after warming to 50 K suggesting that the H_2S ice was amorphous in nature. Around 60 K all H_2S bands sharpened and, in some cases, split and shifted slightly in position. These changes were irreversible and indicated crystallization of the sample. By way of comparison, our spectra at 15 and 90 K resemble published spectra of 9 K amorphous H_2S (Salama et al., 1990) and 88 K crystalline H_2S (Ferraro et al., 1980), respectively. Above 90 K our H_2S samples began to sublime, so that at 100 K only about 10% remained after about 10 min.

Fig. 1b shows IR spectra of pure SO_2 deposited at 16 K and then warmed to 110 K. The 1325 cm^{-1} (ν_3), and 1149 cm^{-1} (ν_1), fundamental bands of SO_2 are as indicated (the 520 cm^{-1} ν_2 fundamental is not shown). Weaker bands at 2457 cm^{-1} ($\nu_1 + \nu_3$) and 2288 cm^{-1} ($2\nu_1$) are more difficult to see in the figure. As with H_2S, the structureless IR features seen at 15 K persisted at 70 K suggesting that the SO_2 sample was amorphous. Around 80 K, the IR bands sharpened and, in some cases, split and shifted slightly in position. These irreversible changes indicated sample crystallization. Above 110 K our SO_2 samples rapidly sublimed. Our spectra are essentially the same as the data of Moore (1984), Salama et al. (1990), and Schriver-Mazzuoli et al. (2003a, 2003b).

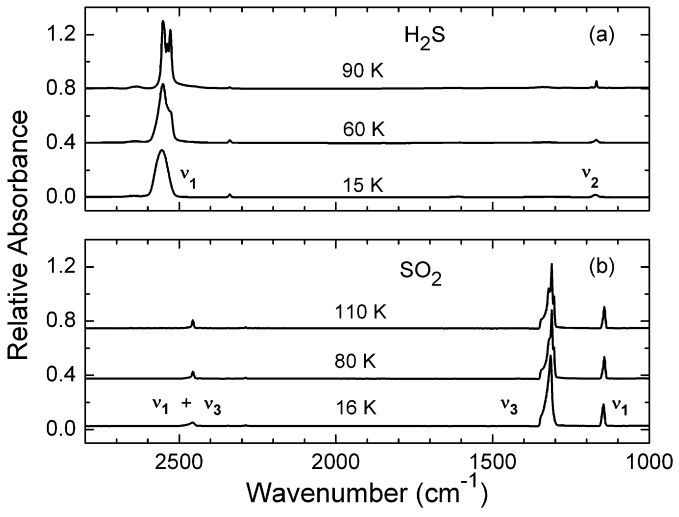

Fig. 1. (a) IR spectra of H_2S deposited at 15 K and subsequently warmed to the temperatures indicated. Spectra share the same vertical scale but are stacked for clarity. (b) IR spectra of SO_2 deposited at 16 K and subsequently warmed to the temperatures indicated. Spectra share the same vertical scale but are stacked for clarity. A very weak feature at 2340 cm^{-1} (4.27 μm) is due to contamination from atmospheric CO_2.

3.1.2. IR spectra of $H_2O + H_2S$ ices

Fig. 2.1 shows IR spectra of an $H_2O + H_2S$ (11:1) ice, formed by co-deposition of H_2O and H_2S at 86 K (Fig. 2.1a) and then warmed to 110 K (Fig. 2.1b) and 132 K (Fig. 2.1c). Four broad features of amorphous H_2O-ice and two bands of H_2S were seen in the 86 K sample, and these are listed in Table 2. Fig. 2.1c shows that after the ice was warmed to 132 K most of the trapped H_2S was gone. As $H_2O + H_2S$ (11:1) samples were warmed beyond the 132 K, the H_2O component

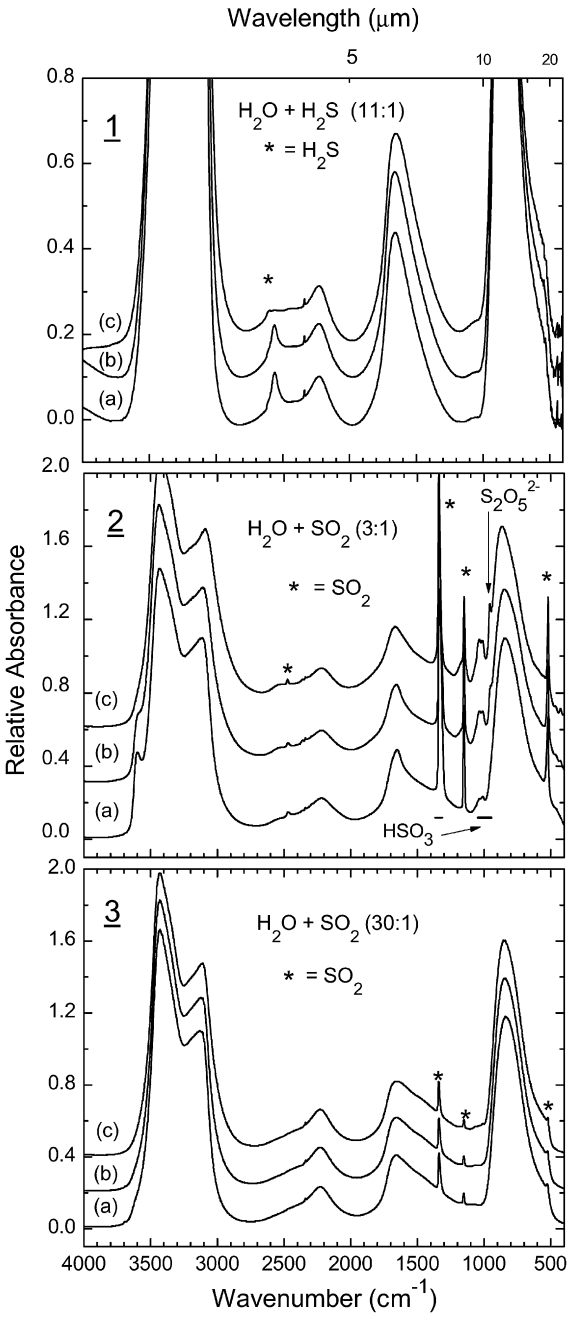

Fig. 2. IR spectra of icy mixtures of: (1) $H_2O + H_2S$ (3:1), (2) $H_2O + SO_2$ (3:1), and (3). $H_2O + SO_2$ (30:1). Each set shows spectra of ices deposited at (a) 86 K and subsequently warmed to (b) 110 and (c) 132 K. Within each set, spectra share the same vertical scale but are stacked for clarity. A weak feature at 2340 cm^{-1} (4.27 μm) is due to contamination from atmospheric CO_2.

showed evidence of crystallization near ~150 K, and sublimed completely from the substrate around 175 K. Mid-IR spectra of more-dilute $H_2O + H_2S$ mixtures, such as 30:1, were dominated by the broad features of amorphous H_2O-ice and are not shown. In no case was a thermally-induced reaction product seen for any $H_2O + H_2S$ mixture.

3.1.3. IR spectra of $H_2O + SO_2$ ices

Fig. 2.2 shows the mid-IR spectra of $H_2O + SO_2$ (3:1) ice at 86, 110, and 132 K. Broad absorption features of amorphous H_2O-ice and four bands of SO_2 can be identified. Band positions are listed in Table 3 for samples made at 86 K and either maintained at 86 K, or warmed to 110 or 132 K. IR spectra of a more-dilute $H_2O + SO_2$ (30:1) mixture are shown in Fig. 2.3 at 86, 110, and 132 K. The ν_3, ν_1, and ν_2 bands of SO_2 can still be seen, but the broad features of amorphous H_2O-ice dominate the spectra. Band positions are again listed in Table 3.

We note three small features around 1035, 1011, and 956 cm^{-1} (9.66, 9.89, and 10.5 μm) in Fig. 2.2. These were observed in $H_2O + SO_2$ (3:1) ices either made at ~86 K or made near 15 K and then warmed to ~86 K. These bands grew as the temperature was increased from 86 to 132 K, after which they were rapidly lost as the sample was further warmed. These bands, which were not present in either pure H_2O, pure SO_2, or $H_2O + SO_2$ (30:1) mixtures, resemble small features observed by Fink and Sill (1982) in an $H_2O + SO_2 + CO_2$ (1:4:1) ice and by Zhang and Ewing (2002) in $H_2O + SO_2$ ices and in liquid-phase solutions. Guided by their work, we suggest that the absorbances at 1035 and 1011 cm^{-1} in Fig. 2.2 probably are due to the bisulfite ion (HSO_3^-) and either one of its reaction products or an isomer. The absorbance near 956 cm^{-1} is probably from $S_2O_5^{2-}$, *meta*-bisulfite (Pichler et al., 1997).

Table 2
Wavenumber positions (cm^{-1}), with wavelengths (μm) beneath in parentheses, for unirradiated $H_2O + H_2S$ (11:1) ices at 86, 110, and 132 K

Identification	86 K	110 K	132 K
ν_1, ν_3 H_2O	Broad band in 3250 (3.08) region		
ν_1 H_2S	2561	2563	2564, ~2603 (sh)
	(3.90)	(3.90)	(3.90, ~3.80 (sh))
$3\nu_L$ H_2O	2224	2224	2224
	(4.50)	(4.50)	(4.50)
ν_2 H_2O	1651	1646	1638
	(6.06)	(6.08)	(6.11)
ν_2 H_2S	1178	–	–
	(8.49)		
ν_L H_2O	~800	–	–
	(12.5)		

3.2. Irradiated ices—reaction products

3.2.1. Irradiated H_2S and $H_2O + H_2S$ ices-products

Because pure H_2S ices sublimed during irradiations at 86 K, we were forced to perform such experiments at a lower temperature. Fig. 3 shows the ν_1 band of amorphous-phase H_2S at 50 K before and after proton irradiation. As radiation doses accumulated, there was a reduction in the ν_1 band area due to radiolytic destruction of H_2S.

The only radiation product of H_2S identified was hydrogen persulfide, H_2S_2, with band assignments based on matrix-isolation studies by Isoniemi et al. (1999). In Fig. 3, the 2485 cm^{-1} (4.02 μm) absorption is attributed to overlapping ν_1

Table 3
Wavenumber positions (cm^{-1}), with wavelengths (μm) beneath in parentheses, for unirradiated $H_2O + SO_2$ ices at 86, 110, and 132 K

Identification	$H_2O + SO_2$ (3:1)			$H_2O + SO_2$ (30:1)		
	86 K	110 K	132 K	86 K	110 K	132 K
OH dangling bonds	3606	3605	–	3693	–	–
	(2.78)	(2.74)		(2.71)		
ν_1, ν_3 H_2O		~3250, broad			~3250, broad	
		(~3.08, broad)			(~3.08, broad)	
$\nu_1 + \nu_3$ SO_2	2471	2471	2474	–	–	–
	(4.05)	(4.05)	(4.04)			
$3\nu_L$ H_2O	2218	2218	2218	2229	2229	2229
	(4.51)	(4.51)	(4.51)	(4.49)	(4.49)	(4.49)
ν_2 H_2O	1652	1657	1668	1656	1656	1655
	(6.50)	(6.04)	(6.00)	(6.06)	(6.06)	(6.04)
ν_3 SO_2	1336	1336	1339	1338	1339	1341
	(7.48)	(7.49)	(7.47)	(7.47)	(7.47)	(7.46)
ν_1 SO_2	1151	1151	1150	1152	1152	1151
	(8.69)	(8.69)	(8.70)	(8.68)	(8.68)	(8.69)
HSO_3^-	~1035, ~1011	~1035, ~1011	~1035, ~1011	1070–1060	1066	1064
	(9.66, 9.89)	(9.66, 9.89)	(9.66, 9.89)	(9.35–9.43)	(9.38)	(9.40)
$S_2O_5^{2-}$	–	956	958	–	–	–
		(10.5)	(10.4)			
ν_L H_2O	843	848	864	834	846	848
	(11.9)	(11.8)	(11.6)	(12.0)	(11.8)	(11.8)
ν_2 SO_2	521	521	519	522	521	521
	(19.2)	(19.2)	(19.3)	(19.2)	(19.2)	(19.2)

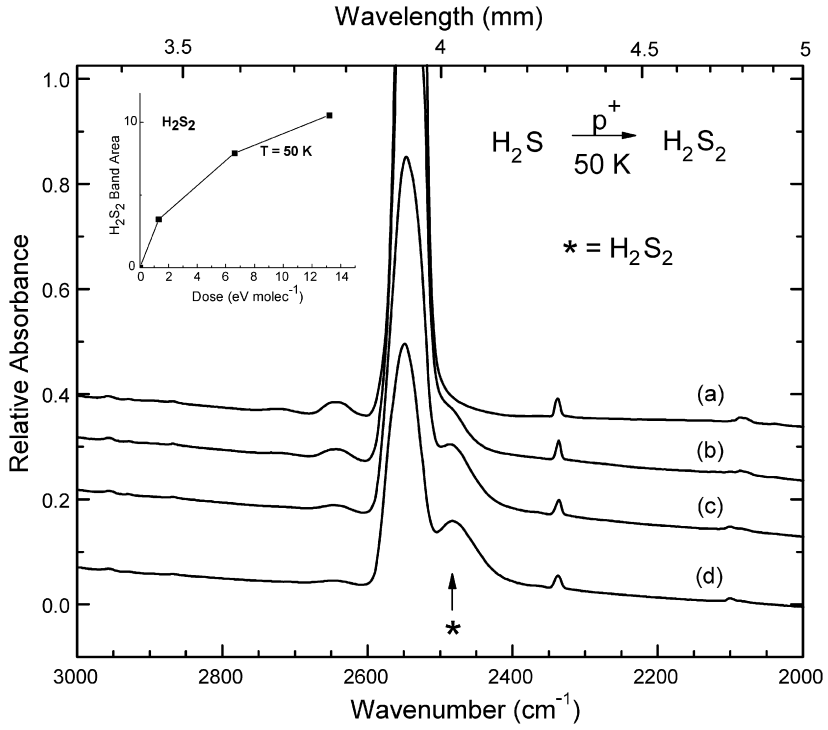

Fig. 3. The ν_1 band of amorphous H_2S at 50 K before (a) and after irradiation to doses of (b) 1, (c) 7, and (d) 13 eV molec^{-1} with 0.8 MeV protons. Spectra share the same vertical scale, but are stacked for clarity. The increase in H_2S_2 band area as a function of dose is shown as an insert. A weak feature at 2340 cm^{-1} (4.27 μm) is due to contamination from CO_2.

and ν_5 features of H_2S_2, the HS symmetric and anti-symmetric vibrations respectively. The increase in the H_2S_2 band area as a function of dose is shown in the plot inserted into Fig. 3. The H_2S_2 band area was extracted by fitting the complex H_2S–H_2S_2 band with two Gaussian curves (Grams software package, Thermo Scientific, Waltham, MA, USA). Typical fits gave a correlation coefficient (R^2) of 0.997.

A much-weaker H_2S_2 absorption was detected at 877 cm^{-1} (11.40 μm), probably due to HSS bending (spectrum not shown). On warming the irradiated H_2S ice to 180 K the 2485 cm^{-1} band of H_2S_2 remained, showing that the vapor pressure of H_2S_2 was lower than that of H_2S, as expected.

Fig. 4 shows spectra of $H_2O + H_2S$ (8:1) ice at 86 K before and after proton irradiation. New features are identified with H_2S_2 and SO_2, and band positions are given in Table 4. An expansion of the 2550 cm^{-1} region shows changes in the H_2S and H_2S_2 bands as a function of dose. For observers, H_2S_2 may be detectable as a long-wavelength wing on the H_2S band at 2561 cm^{-1} (3.90 μm). Its formation, as part of the radiolytic sulfur cycle, competes for and removes sulfur that would take part in oxidation. SO_2 was also identified in similar $H_2O + H_2S$ mixtures irradiated at 110 and 132 K, but H_2S_2 was not detected. H_2S features were extremely weak in $H_2O + H_2S$ ($\geqslant$30:1) ices and features of radiation products could not be measured. Finally, in no case was H_2O_2 observed in any of our irradiated $H_2O + H_2S$ mixtures.

3.2.2. *Irradiated SO_2 and $H_2O + SO_2$ ices-products*

Irradiated SO_2-ice was studied by Moore (1984) at 20 and 88 K, and the main reaction product detected was SO_3. A sample spectrum of pure amorphous SO_2-ice at 50 K before and after irradiation (dose = 10 eV molec^{-1}) is shown at the bottom of Fig. 5. Comparing these spectra with irradiated $H_2O + SO_2$ (3:1) ice at 86 K (Fig. 5d), demonstrates that SO_3 is not detected when SO_2 is diluted in H_2O. The four IR traces of $H_2O + SO_2$ correspond to (a) unirradiated ice and radiation doses of (b) 1, (c) 5, and (d) 15 eV molec^{-1}. Spectrum (b), after only 1 eV molec^{-1}, shows the growth of a band at 1037 cm^{-1} (9.64 μm) attributed to bisulfite, HSO_3^- (Zhang and Ewing, 2004). This feature, along with a weak companion in the 1250 cm^{-1} (8.00 μm) region, continued to grow with increasing dose. Sulfate, SO_4^{2-}, was also found, seen in Fig. 5 after 5 eV molec^{-1} with features at 1110, 982, and ~611 cm^{-1} (9.01, 10.2, and 16.4 μm), similar to positions reported by Querry et al. (1974). As with HSO_3^-, the SO_4^{2-} features increased with additional irradiation. Moving to Fig. 5c and Fig. 5d, an IR feature of H_3O^+ is found at 1724 cm^{-1} (5.80 μm) with an intensity sufficient to broaden the 1650 cm^{-1} H_2O band (Carlo and Grassian, 2000). An increase in a blended feature near 1052 cm^{-1} (9.51 μm), and possibly some of the growth in the 1250 cm^{-1} region, are assigned to the bisulfate ion, HSO_4^- (Horn and Sully, 1999). All band positions for ions observed are listed in Table 4.

A water irradiation product, H_2O_2, showed a weak broad band near 2860 cm^{-1} in the $H_2O + SO_2$ (3:1) ice irradiated at 86 K. The H_2O_2 band was not specifically measured, but it can be estimated by comparison with data from our previous H_2O_2 work (Moore and Hudson, 2000). This comparison leads to not more than a few tenths of a percent H_2O_2 being made in irradiated $H_2O + SO_2$ (3:1) mixtures. In ices irradiated at higher

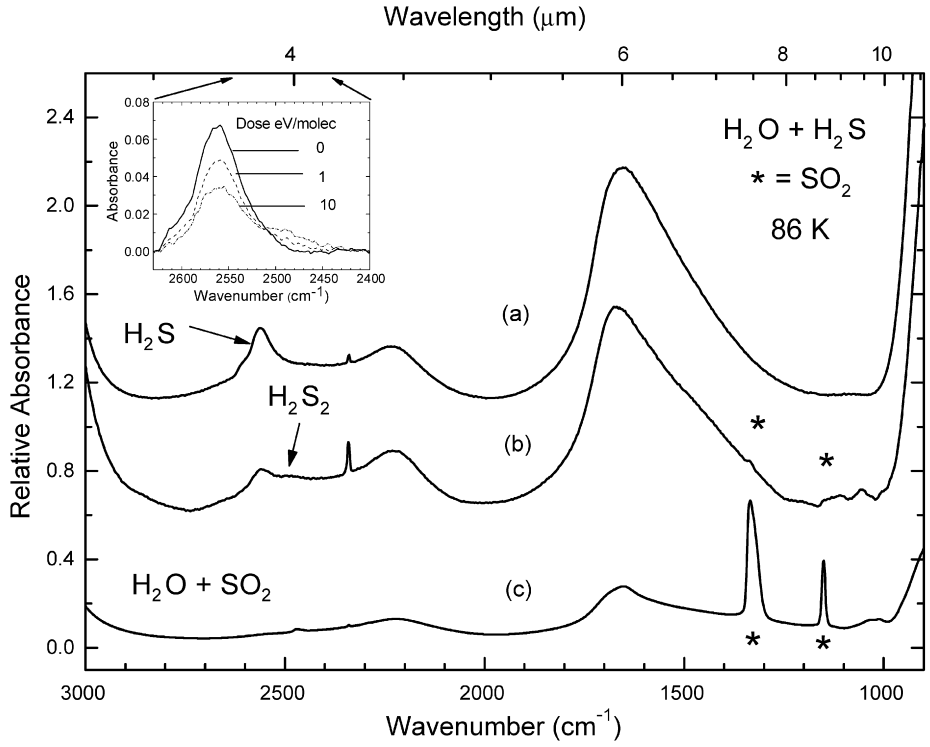

Fig. 4. IR spectra of an $H_2O + H_2S$ (8:1) ice before (a) and after (b) proton irradiation to a dose of 15 eV molec^{-1} at 86 K. Asterisks mark weak features indicating SO_2 formation. For comparison, a spectrum of $H_2O + SO_2$ ($H_2O/SO_2 = 3$) at 86 K is shown in (c). Spectra are offset for clarity. A weak feature at 2340 cm^{-1} (4.27 μm) is due to contamination from CO_2. Insert spectra expand the 2550 cm^{-1} region, showing the ν_1 H_2S band changes from 0 to 10 eV molec^{-1} and the formation of the H_2S_2 shoulder.

Table 4
Wavenumber positions (cm^{-1}), with wavelength (μm) beneath in parentheses, for radiation products identified in ices at 86, 110, and 132 K, unless noted

$H_2O + H_2S$ (8:1)		$H_2O + SO_2$ (3:1)		$H_2O + SO_2$ (30:1)[a]	
Product	Position	Product	Position	Product	Position
–	–	H_2O_2	∼2811 (3.56)	–	–
H_2S_2[b]	2490 (4.02)	H_3O^+	1724 (5.80)	–	–
SO_2	1335 and 1151 (7.49 and 8.69)	HSO_3^-	1235 region and 1037 (8.1 and 9.64)	–	–
–	–	HSO_4^-	1235 region and 1052 (8.1 and 9.51)	HSO_4^-	1235 region and 1052 (8.1 and 9.51)
–	–	SO_4^{2-}	∼1110, 982, and ∼611 (9.01, 10.2 and 16.4)	SO_4^{2-}	∼1110 and 611 (9.01 and 16.4)

[a] Evidence for these ions was also found in $H_2O + SO_2$ (10:1) irradiated at 86 K.
[b] H_2S_2 was detected only when the ice was irradiated at 86 K.

temperatures, or in those with a lower initial concentration of SO_2, this H_2O_2 feature was not detected. It is thought that this oxidant plays a role in the formation of sulfur products we observe, and this role will be considered in Section 4.

3.3. Irradiated ices—Destruction of SO_2 and H_2S

The radiation destruction of SO_2 was measured at 86, 110, and 132 K for ices initially having $H_2O/SO_2 = 3$ and 30. Fig. 6 plots the normalized area of the ν_1 SO_2 band (1151 cm^{-1}, 8.69 μm) as a function of absorbed dose. The figure shows that the rate of decrease of the ν_1 band depends on both temperature and the initial H_2O/SO_2 ratio. At higher doses the SO_2 concentration is non-zero. A first-order exponential decay fit to the $H_2O/SO_2 = 30$ cases, presumed to be similar to Europa, give plateau levels of 0.036, 0.029, and 0.040 for the 86, 110, and 132 K irradiations, respectively. At smaller doses, the SO_2 band area decreases by 50% for 1.8, 4.9, and 9.2 eV molec^{-1} for $H_2O/SO_2 = 3$ ices at 86, 110, and 132 K, respectively. In the $H_2O/SO_2 = 30$ mixture, half of the SO_2 is lost with doses under 1 eV molec^{-1}. The top axis in Fig. 6 relates these doses to those expected for Europa's near-IR-sensed 100-μm surface layer, for which it is estimated that 1 eV molec^{-1} accumulates per year (Cooper et al., 2001). The time required to destroy half the original SO_2 is, of course, the radiation half-life that refers to the early part of the irradiations before product formation is

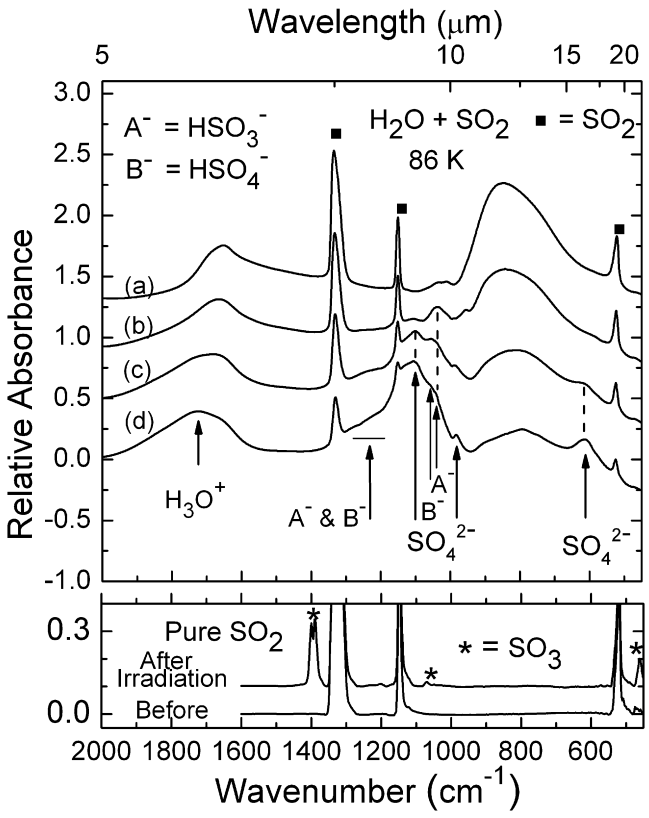

Fig. 5. IR spectra of an $H_2O + SO_2$ (3:1) ice before (a) and after irradiation to doses of (b) 1, (c) 5, and (d) 15 eV molec^{-1} with 0.8 MeV protons at 86 K. For comparison, spectra of pure SO_2 before and after irradiation also are shown. Spectra share the same vertical scale but are stacked for clarity.

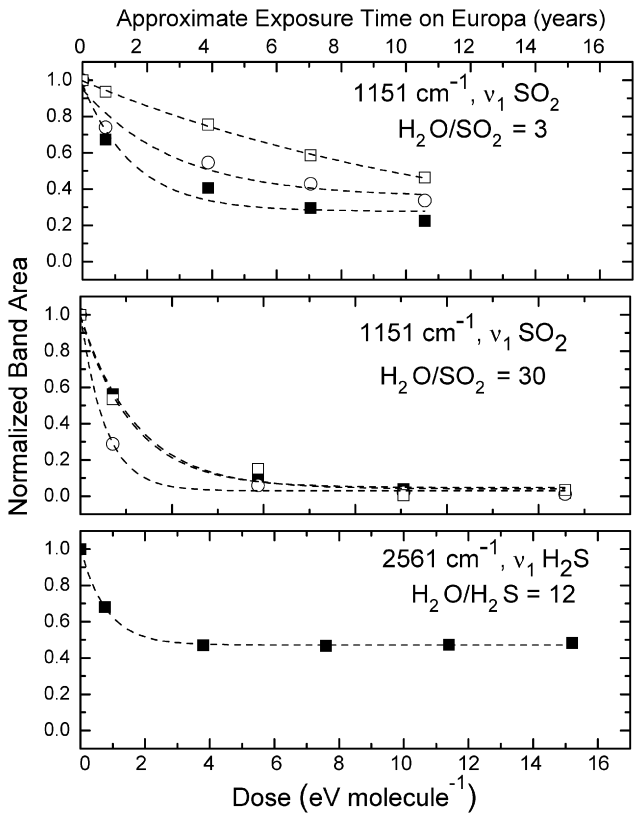

Fig. 6. Normalized areas of sulfur IR bands in H_2O-dominated ices as a function of dose in eV molec^{-1}. Data are given for 86 K (■), 110 K (○), and 132 K (□). The upper x-axis shows the time required to accumulate an equivalent laboratory dose in the top 100-μm layer of surface material on Europa (from Cooper et al., 2001). Least-squares fits of a first-order exponential decay are shown for the data.

significant and back reactions become important. Table 5 lists our measured half-lives for Europa, Ganymede, and Callisto ices initially having $H_2O/SO_2 = 3$ and 30 ratios and maintained at 86, 110, or 132 K.

For comparison with our SO_2 destruction data, an attempt was made to assess the radiation stability of H_2S in H_2O-rich ices by measuring the decay of the largest H_2S IR band (ν_1). Fig. 6 plots this decay, for an ice with an initial ratio of $H_2O/H_2S = 11$ at 86 K. We determined that about 50% of the H_2S remained in the ice after a dose of about 2.2 eV molec^{-1}. Since the ν_1 2452 cm^{-1} H_2S band overlapped with a dominant radiation product, H_2S_2, with a band center at 2490 cm^{-1} (see insert spectra, Fig. 4), curve-fitting techniques (Grams software, Gaussian profiles) again were used to extract the decreasing band area of H_2S with dose. Correlation coefficients for fits were typically around 0.997. As already mentioned, the H_2S bands were very weak in $H_2O + H_2S$ ($\geqslant$30:1) ices, and were thermally unstable over several hours in 110 K ices, prohibiting their study.

3.4. Irradiated icy mixtures—Thermal evolution

3.4.1. Thermal evolution of irradiated $H_2O + SO_2$ (3:1) ices

Warming irradiated (86 K) $H_2O + SO_2$ ices a few tens of degrees did not cause significant changes in their spectra. IR signatures of SO_4^{2-}, and H_3O^+ (shown in Fig. 5d) were essentially the same for spectra recorded at 86, 110, 132, and 150 K. However, between 150 and 175 K changes occurred as sublimation of the H_2O-matrix material increased. This is illustrated in Fig. 7 where spectra are shown for an irradiated $H_2O + SO_2$ (3:1) ice at 86 K, 175 K, and three higher temperatures. In general, each spectrum can be described in terms of two regions. Broad absorptions are found in the 2000–1500 cm^{-1} (5.0–6.67 μm) region, due largely to H_2O and H_3O^+, while narrower bands, mostly from sulfur-containing ions such as SO_4^{2-}, dominate below 1500 cm^{-1}. Fig. 7a duplicates the spectrum of Fig. 5d, from an irradiated $H_2O + SO_2$ (3:1) ice at 86 K, and Fig. 7b is the same ice warmed during 3.5 h to 175 K under dynamic vacuum conditions. By 175 K, the H_2O matrix had significantly decreased, as shown by the sharpening of the H_3O^+ band at 1724 cm^{-1} (5.80 μm) relative to the diminished low-frequency shoulder due to H_2O. The ν_1, ν_2, and ν_3 SO_2 bands are gone due to sublimation. Relative to the SO_4^{2-} feature at ~1110 cm^{-1} (~9.01 μm), there is an increase in the 1221 cm^{-1} (8.190 μm) band and an increase in the broad low-frequency wing. These changes are consistent with the sample's transformation into crystalline H_2O-ice and H_2SO_4 hydrates, such as the octa-, hemi- and tetrahydrates (40.5, 45.6 and 57.6 weight % H_2SO_4) (Zhang et al., 1993). The unique identification of the more stable tetrahydrate will be discussed in Section 3.4.3. Fig. 7c shows the result of subsequently raising the

Table 5
Estimated radiation-chemical half-lives (years) in top 100 μm of icy satellite surfaces

Satellite	Time to accumulate 1 eV per molecule in top 100 μm[a] (yr)	$H_2O + SO_2$ (3:1)			$H_2O + SO_2$ (30:1)			$H_2O + H_2S$ (11:1)
		86 K	110 K	132 K	86 K	110 K	132 K	86 K
Europa	1	2	5	9	0.9	0.4	0.9	2
Ganymede (pole)	6	12	30	54	5.4	2.4	5.4	12
Ganymede (equator)	80	160	400	720	72	32	72	160
Callisto	140	280	700	1260	126	56	126	280

[a] Depth profiles for total volume dosage rate are from Cooper et al. (2001, Fig. 16).

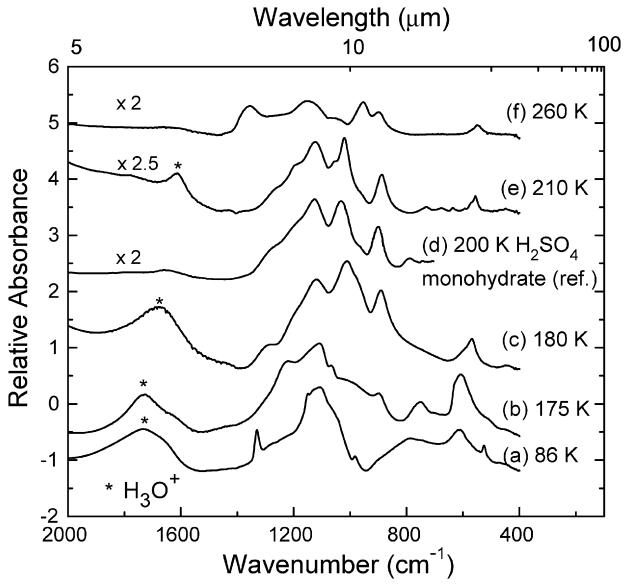

Fig. 7. (a) IR spectra of $H_2O + SO_2$ (3:1) after irradiation to a dose of 15 eV molec^{-1} at 86 K. See Fig. 5d for spectral band identifications. Spectrum (a) evolves with warming, as shown. Reference spectrum (d) is for crystalline H_2SO_4 monohydrate, $H_2SO_4 \cdot H_2O$, at 210 K (Couling et al., 2003, Fig. 1). Spectra have different scaling factors as indicated, and are stacked for clarity.

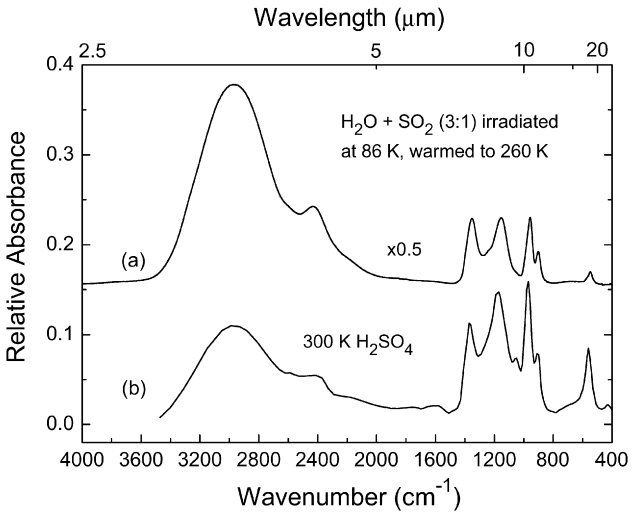

Fig. 8. (a) Reference spectrum of a 0.1-μm film of 95.6 weight % H_2SO_4 at 300 K (see text and Palmer and Williams, 1975). (b) IR spectrum of $H_2O + SO_2$ (3:1) after irradiation at 86 K and subsequent warming to 260 K. Irradiation at either 110 or 132 K and subsequent warming also gave this spectrum. The two spectra are offset for clarity.

temperature only 5 K, to 180 K, and holding it there in a dynamic vacuum for about 24 h. The three major peaks in the 180 K spectrum are at 1119, 1011, and 891 cm^{-1} (8.937, 9.891, 11.2 μm). These peaks shifted but slightly, to 1125, 1020, and 887 cm^{-1} (8.89, 9.80, 11.3 μm), when the ice was warmed to 210 K, as seen in Fig. 7e. Our 180 and 210 K data possess a strong resemblance to the spectrum of 200 K H_2SO_4 monohydrate seen in Fig. 7d, $H_2SO_4 \cdot H_2O$ (Horn and Sully, 1999; Couling et al., 2003), and so are assigned to that crystalline material. (The composition of the monohydrate is 84.5 weight % H_2SO_4.) Dehydration of our $H_2SO_4 \cdot H_2O$ was triggered by an increase in temperature to 260 K, and the spectrum of the residual film is shown in Fig. 7f. The identification of this film as sulfuric acid is discussed in Section 3.4.2. Peak positions, and identifications, of the monohydrate identified with Fig. 7e are summarized in Table 6 along with data for the reference spectrum (Fig. 7d).

3.4.2. Formation and identification of H_2SO_4

Warming irradiated $H_2O + SO_2$ (3:1) ices to 260 K resulted in their dehydration and the formation of a residual film identified as sulfuric acid. Fig. 8a duplicates the 260 K spectrum shown in Fig. 7f and compares this residual material with a reference spectrum of a 0.1-μm liquid film of 96 weight % H_2SO_4 at 300 K, plotted using the optical constants of Palmer and Williams (1975). Peak positions of both spectra are listed in Table 6 along with data for liquid H_2SO_4 at 250 K, discussed by Horn and Sully (1999). The sulfuric acid formed by warming our irradiated ices has a peak pattern similar to the reference data, although positions are shifted slightly. These shifts probably reflect small differences in temperature and concentration. Other experiments in which H_2SO_4 spectra were identified at ~260 K were those with ices having an initial ratio of $H_2O/SO_2 = 3$ (irradiated at 110 and 132 K), $H_2O/SO_2 = 10$ (irradiated at 86 K), and $H_2O/\{SO_2 + CO_2\} = 1.5$ (irradiated at 77 and 110 K). More-dilute mixtures with $H_2O/SO_2 = 30$, did not result in a detectable IR signature of H_2SO_4. Based on the SO_3–H_2O–H_2SO_4 phase diagram (Gable et al., 1950), and the temperatures and pressures used in these experiments, it is likely that our residual sulfuric acid film is a solid.

3.4.3. Formation and identification of sulfuric acid tetrahydrate, $H_2SO_4 \cdot 4H_2O$, from H_2O + (SO_2 or H_2S) = 10–30 ices

A residual film whose IR spectrum was identified as sulfuric acid tetrahydrate, $H_2SO_4 \cdot 4\ H_2O$, was formed when irradi-

Table 6
Wavenumber positions (cm^{-1}), with wavelengths (μm) beneath in parentheses, for products in ices after irradiation and warming

Tetrahydrate, this work, 170–190 K	Tetrahydrate, reference,[a] 143 K	Tetrahydrate, reference,[b] 180 K	Tetrahydrate, (see Fig. 9) identification ion (mode)[b]	Monohydrate, this work, 210 K	Monohydrate, reference,[c] 190 K	Monohydrate, (see Fig. 7) identification ion (mode)[c]	Sulfuric acid, this work, 250–260 K	Sulfuric acid, reference,[d] liquid, 95.6%, 300 K	Sulfuric acid, reference,[c] liquid, 250 K	Sulfuric acid, (see Fig. 8) identification (mode)
~3057	3300–2800	3230	Water ice st				2945	2990	2950	$\nu_{as}S(O–H)_2$
(3.27)	(3.03–3.57)	(3.10)					(3.39)	(3.34)	(3.39)	$\nu_sS(O–H)_2$
~2820		2840	H_3O^+ &	2852	2860	H_3O^+	2425	2410	2420	
(3.55)		(3.52)	$H_5O_2^+$ st	(3.51)	(3.45)	(ν_{as}, ν_sO–H)	(4.12)	(4.15)	(4.13)	
~2230	2450–2250	2270	H_3O^+ overtone/	2157	2202	Overtone/	–	–	–	
(4.48)	(4.08–4.44)	(4.41)	combination	(4.63)	(4.54)	combination				
1705	1725	1718	H_3O^+	1611	1699	H_3O^+	–	–	–	
(5.87)	(5.80)	(5.82)	(δH_3O^+)	(6.21)	(5.89)	(δH_3O^+)				
1429	–	–	–	–	–	–	–	–	–	
(6.70)										
1220	–	1220	–	–	–	–	1351	1370	1361	ν_{as}(O=S=O)
(8.20)		(8.20)					(7.40)	(7.30)	(7.35)	
–	–	1153	SO_4^{2-}	1122	1130	HSO_3^-	1151	1170	1159	$\delta S(O–H)_2$
		(8.68)	($\nu_{as}SO_3$)	(8.91)	(8.85)	($\nu_{as}SO_3$)	(8.69)	(8.55)	(8.63)	
1074	1077	1074	SO_4^{2-}	1050	–	–	–	–	–	–
(9.31)	(9.29)	(9.31)	($\nu_{as}SO_4$)	(9.52)						
1014	–	1039	SO_4^{2-}	1020	1034	HSO_3^-	958	970	965	ν_{as}(S–(OH)$_2$)
(9.86)		(9.62)	($\nu_{as}SO_3$)	(9.80)	(9.67)	(ν_sSO_3)	(10.4)	(10.31)	(10.4)	
885	–	900	SO_4^{2-}	886	902	HSO_3^-	902	910	905	ν_s(S-(OH)$_2$)
(11.3)		(11.1)	(Overtone?)	(11.3)	(11.1)	(ν_sO_3S-OH)	(11.1)	(10.99)	(11.1)	
749	–	–	–	–	–	–	–	–	–	–
(13.4)										
~596	–	600	SO_4^{2-}	556	599	(δSO_3?)	547	–	–	–
(16.8)		(16.7)	(δSO_4)	(18.0)	(16.7)		(18.3)			

[a] Zhang et al. (1993).
[b] Nash et al. (2000).
[c] Horn and Sully (1999).
[d] Palmer and Williams (1975).

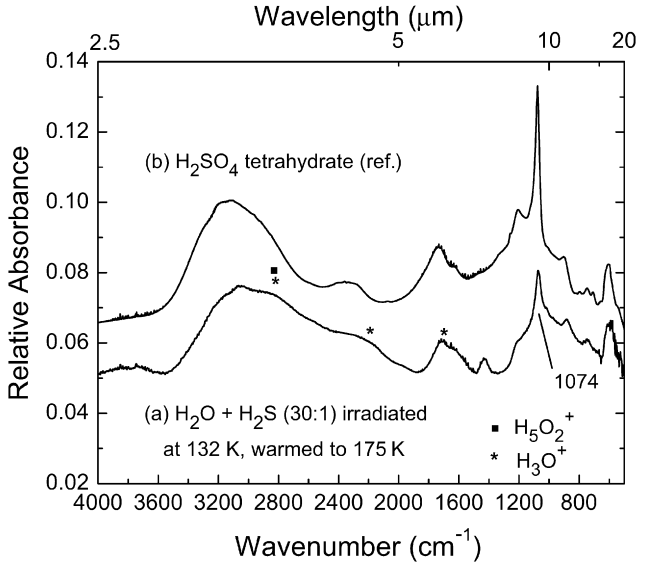

Fig. 9. (a) IR spectrum of irradiated $H_2O + H_2S$ (initially 30:1) warmed to ~175 K, compared with (b) a reference spectrum of crystalline H_2SO_4 tetrahydrate, $H_2SO_4{\cdot}4H_2O$ (Zhang et al., 1993) at 195 K. Table 6 lists the peak positions. The two spectra are offset for clarity.

ated ices with initial ratios of $H_2O/SO_2 = 30$, $H_2O/SO_2 = 10$, and $H_2O/H_2S > 30$ were warmed to 188, 175–179 K, and 175 K, respectively. Fig. 9 compares the spectrum of irradiated $H_2O/H_2S > 30$ at 175 K with a reference spectrum of the tetrahydrate at 195 K (Zhang et al., 1993). Table 6 lists peak positions for these spectra, comparison data from Nash et al. (2000), and band identifications for the tetrahydrate. Both spectra in Fig. 9 possess broad bands at 3300–2800 cm^{-1} (3.030–3.571 μm), due to H_3O^+ and $H_5O_2^+$, and 1725 cm^{-1} (5.80 μm), due to H_3O^+ (Nash et al., 2000). The sharp feature at 1077 cm^{-1} (9.285 μm) is due to SO_4^{2-}, as is the absorption near 596 cm^{-1} (16.7 μm). In a different experiment, slowly warming irradiated $H_2O + SO_2$ (10:1) ice gave $H_2SO_4{\cdot}4H_2O$ near 175 K, and with additional dehydration the spectrum of H_2SO_4 was obtained at ~260 K (spectrum not shown).

4. Discussion

4.1. Reactions and mechanisms

4.1.1. Irradiated pure H_2S and SO_2 ices

We have identified H_2S_2 in irradiated H_2S-ice, at both 12 and 50 K. By analogy with H_2O, during radiolysis H_2S can dissociate into either H atoms and SH radicals or into H_2 and the S atom. Both H and HS can undergo radical–radical reactions to either reform H_2S or to make H_2 and H_2S_2. Therefore, the

reactions to make H_2S_2 from H_2S likely resemble those for the formation of H_2O_2 from H_2O:

$$H_2S \rightarrow H + HS,$$

$$H + H \rightarrow H_2,$$

$$HS + HS \rightarrow H_2S_2.$$

Our detection of H_2S_2 is consistent with an earlier photochemical study of pure H_2S (Salama et al., 1990) in which the growth of a weak unidentified shoulder on the low-energy side of the ν_1 H_2S band, consistent with H_2S_2 formation, was noted. We have also observed H_2S_2 in experiments with H_2O-rich ice mixtures, such as $H_2O/H_2S = 8$–12 irradiated at 86 K. This suggests that the above reactions continued to operate even when the H_2S was diluted, although the lower yield of H_2S_2 indicates that the presence of H_2O hindered the dimerization of HS radicals.

For irradiations of pure SO_2, it has long been known (Moore, 1984) that the main product seen in the infrared spectrum is SO_3. The relevant reactions appear to be

$$SO_2 \rightarrow SO + O,$$

$$SO_2 + O \rightarrow SO_3.$$

This sequence has the support of matrix-isolation experiments (Schriver-Mazzuoli et al., 2003b).

4.1.2. *Irradiated icy mixtures—$H_2O + H_2S$ and $H_2O + SO_2$*

Turning now to mixtures, our irradiated $H_2O + H_2S$ samples produced SO_2, while our $H_2O + SO_2$ samples produced distinct bands of H_3O^+ and SO_4^{2-}. This suggests that the overall change is one of sulfur oxidation, summarized as follows:

$$H_2O + H_2S \rightarrow H_2O + SO_2 \rightarrow \left\{H_3O^+ \text{ and } SO_4^{2-}\right\}.$$

Each of our irradiated mixtures fell into this sequence, whether the initial ratio of water-to-sulfur-molecule was 3:1, 30:1, or something in between. For the second step of the above sequence, the ions produced were trapped in the amorphous ice until the sample was warmed, at which point irreversible changes took place to make sulfuric acid hydrates and eventually, in some cases, sulfuric acid.

The initial step of the above sequence, oxidation of H_2S to SO_2 has been studied by others. Liuti et al. (1966) examined gas-phase H_2S oxidation by O atoms, and found the following effective:

$$H_2S + O \rightarrow HS + OH,$$

$$HS + O \rightarrow SO + H.$$

From matrix-isolation experiments, Tso and Lee (1984) argued that O-atom reactions are not as important as those involving HO_2 radicals. For example, many processes other than the above, such as direct radiolytic dissociation of H_2S, can give HS. This radical can then react with HO_2 from the irradiated H_2O-ice:

$$HS + HO_2 \rightarrow SO + H_2O.$$

In other words, both gas-phase and condensed-phase experiments agree on the formation of the SO molecule. In our experiments, this species will be converted to SO_2 by reaction with O atoms from irradiated H_2O-ice:

$$SO + O \text{ (from } H_2O) \rightarrow SO_2.$$

Alternatively, O-atom transfer with SO might be important:

$$SO + SO \rightarrow SO_2 + S.$$

Other reactions are certainly possible, but the above are likely contributors to the SO_2 we observe in irradiated $H_2O + H_2S$ mixtures.

The simplest way to interpret the subsequent reactions of SO_2 in H_2O-ice is to assume that SO_3 is also made, albeit at a much lower level than in the irradiation of pure anhydrous SO_2. The reaction of SO_3 with H_2O has essentially no barrier in a water matrix (Larson et al., 2000), and would give the H_3O^+ and HSO_4^- ions we observed:

$$2H_2O + SO_3 \rightarrow H_3O^+ + HSO_4^-.$$

As the HSO_4^- abundance rises on continued irradiation, the extent of

$$HSO_4^- + H_2O \rightarrow H_3O^+ + SO_4^{2-},$$

is expected to increase, leading to the growth in SO_4^{2-} seen in Fig. 5.

Another way for SO_2 to be converted into SO_4^{2-} is through a reaction sequence similar to that operative in terrestrial clouds (Chandler et al., 1988; Clegg and Abbatt, 2001):

$$H_2O + SO_2 \rightarrow H^+ + HSO_3^-,$$

$$HSO_3^- + H_2O_2 \rightarrow HSO_4^- + H_2O,$$

$$HSO_4^- + H_2O \rightarrow H_3O^+ + SO_4^{2-}.$$

This sequence has the advantage of explaining the IR bands we observe in positions for HSO_3^- and HSO_4^-. The oxidizing agent used is H_2O_2, a known product of H_2O-ice irradiation.

Yet another possible source of SO_2, and from there SO_4^{2-}, is the successive oxidation of elemental sulfur by OH radicals. This pathway may be more relevant to Europa's sulfur cycle than to our experiments, since ices in the latter do not contain elemental sulfur. See Carlson et al. (2002) and references therein for information on the pertinent reactions.

Fig. 10 summarizes some of these reactions leading from H_2S to SO_4^{2-} at 86 K and above. Solid arrows indicate observed transformations while dashed arrows indicate those which seem reasonable but require additional work to confirm. Note that free radical paths are not included in this figure. For example, one could envision free-radical processes such as the consecutive addition of OH radicals, from H_2O radiolysis, to SO_2:

$$OH + SO_2 \rightarrow HSO_3,$$

$$OH + HSO_3 + H_2O \rightarrow H_3O^+ + HSO_4^-,$$

$$HSO_4^- + H_2O \rightarrow H_3O^+ + SO_4^{2-}.$$

However, since we are unaware of efficient, consecutive OH additions in solid-phase radiation chemistry we do not favor this set of reactions.

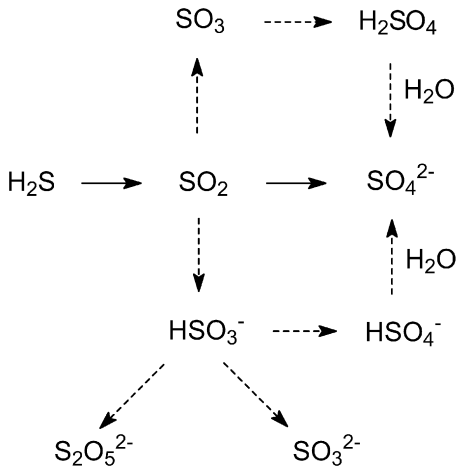

Fig. 10. Schematic of reactions summarizing the conversion of H_2S into SO_2, various ions, and sulfuric acid.

4.2. Radiation destruction of SO_2 and H_2S in H_2O ices

We have used SO_2 infrared bands in H_2O-ice mixtures to determine the destruction rate of this molecule as a function of radiation dose, temperature, and ice composition. In general, the destruction rate of SO_2 for $H_2O + SO_2$ (3:1) ices varied inversely with temperature (Fig. 6), probably due to recombination of radicals at the higher temperatures to reform SO_2. Based on our experiments, the SO_2 destruction rate also was related inversely to the initial SO_2 concentration. Understanding the underlying mechanisms for this may require more detailed studies, but the trend supports the idea that there is an increased probability of attack by H and OH radicals in the more H_2O-rich ices. Table 5 shows that the estimated half-life of SO_2 on Europa (in the absence of any sources) is 2–9 years for $H_2O/SO_2 = 3$ ices at 86 and 132 K, and less than 1 year for $H_2O/SO_2 = 30$ ices over that temperature range.

At a concentration of $H_2O/H_2S = 11$, the destruction half-life of H_2S was 2 years, similar to that of SO_2 in an $H_2O/SO_2 = 3$ ice at 86 K. Comparing the destructions in Fig. 6, after ~10 years of estimated exposure on Europa, the SO_2 concentration is still decreasing in ices initially having $H_2O/SO_2 = 3$, and it has reached a plateau of about 0.1% SO_2 for ices initially having $H_2O/SO_2 = 30$. In the $H_2O + H_2S$ sample, the H_2S concentration has leveled out at about 50% of its original value. This probably reflects a near balance between the ongoing destruction of H_2S and its reformation from HS and H atoms, the latter originating either from the H_2O-ice matrix or from H_2S itself.

4.3. Dehydration of irradiated ices on warming, and the formation of hydrates and sulfuric acid

The IR spectra in Fig. 7 reveal the changes triggered by warming an irradiated $H_2O + SO_2$ (3:1) mixture. The 86 K spectrum shows that the sample was a mixture of ions embedded in amorphous H_2O-ice and residual SO_2. By 175 K the sample was crystallizing into a sulfuric acid hydrate, probably the tetrahydrate or octahydrate, the two having similar spectra (Zhang et al., 1993). As the sample sat at 180 K under a dynamic vacuum for 24 h, it lost sufficient H_2O to convert to sulfuric acid monohydrate (Couling et al., 2003), which remained the stable form of the sample to 210 K. At that temperature, the spectral bands decreased, consistent with a loss of H_2O and a combination of ions. Compare, for example, the H_3O^+ bands near 1700 cm^{-1} at 180 K and 210 K.

For irradiated ices with H_2O:SO_2 ratios of 10 and 30, and for several $H_2O + H_2S$ mixtures, a spectrum of sulfuric acid tetrahydrate was recorded when the sample was slowly (over ~1 h) warmed through the 175–188 K temperature range. During this warming period, typical IR spectra were different from the spectra shown in Figs. 7a and 7b (for H_2O:SO_2 ratio of 3) because they were dominated by stronger absorptions of H_2O. Formation of the tetrahydrate, as opposed to the monohydrate obtained from $H_2O + SO_2$ (3:1) mixtures, is reasonable. Insufficient sulfur species were available to react with all of the H_2O-ice available. Once formed, the tetrahydrate dehydrated with additional warming, making H_2SO_4.

To summarize our warming experiments, the observed trend was for irradiated ices to lose H_2O with increasing temperature and to become richer in H_2SO_4, as outlined below:

$$H_2O + H_2S \rightarrow H_2O + SO_2 \rightarrow H_3O^+, SO_4^{2-}, HSO_4^-$$
(by radiolysis),

$$\{H_3O^+,\ SO_4^{2-},\ HSO_4^-\} \rightarrow H_2SO_4 \text{ hydrate(s)} \rightarrow \text{pure } H_2SO_4$$
(by warming).

This trend agrees with the work of Nash et al. (2000) who reported the dehydration of sulfuric acid tetrahydrate to sulfuric acid monohydrate at 180 K under vacuum. Our results also are consistent with those of Zhang et al. (1993) who observed, for example, that 47.6 weight % H_2SO_4 solutions evolve from a crystalline hemihydrate, $H_2SO_4 \cdot 6.5H_2O$, at 210–219 K to a tetrahydrate plus liquid H_2SO_4 at ~220 K. In addition, we observed that CO_2 added into the original irradiated ice mixture (H_2O:SO_2:CO_2 = 3:1:1) did not prevent the formation of sulfuric acid through competing reactions.

5. Relevance to the Galilean satellite surfaces

The overall principal chemical result of our experiments is that the sulfur-containing molecules in ices relevant to Europa are oxidized with radiation processing. Both H_2S and SO_2 undergo radiation chemical reactions that change their sulfur oxidation state from −2 and +4, respectively, to +6 (in the form of SO_4^{2-}). The formation of SO_4^{2-} from SO_2 in H_2O is part of Europa's radiolytic sulfur cycle (Carlson et al., 1999a, 1999b, 2002) and results in the net production and diffusive loss of hydrogen. During the formation of SO_4^{2-}, atomic oxygen (a radiation product) is used and these reactions compete with other paths that produce O_2 (Johnson et al., 2005). The SO_4^{2-} ion, in the form of H_2SO_4, and H_2O_2 are less volatile than the other observed oxidants on Europa, O_2 and CO_2. Together, the presence of these oxidants increases the likelihood that the decomposition of any organics and salts will be enhanced (Johnson et al., 1998).

Our laboratory results show that radiolysis of SO_2 in H_2O-ice at Europa's temperature produces both anions (SO_4^{2-}, HSO_3^-, and HSO_4^-) and cations (H_3O^+ and $H_5O_2^+$) where these "free ion" pairs are distributed throughout the bulk of the ice. On the time scales of our experiments, these species appeared stable in the 86–150 K range. Similar ions formed on the surfaces of the icy satellites may move to a lower energy state with time, evolving into a mixture of sulfuric acid crystalline hydrates and crystalline ice. Carlson et al. (2005) noted that Europa's hydrate spectrum could be described as a mixture of random (liquid-like) and ordered (crystalline) sulfuric acid anions and cations. Radiolysis produces a random ion distribution that may slowly form crystalline hydrates, only to be destroyed by irradiation in the continuing sulfur cycle.

The detection of H_3O^+ in these experiments, both as "free H_3O^+" found in irradiated $H_2O + SO_2$ ices, and "ordered H_3O^+" associated with the hydrates, demonstrates its radiation formation and thermal stability. This ion, along with radiation-formed H_2O_2, were proposed to describe Europa's "non-icy" spectrum (Clark, 2004). More work on the spectra of irradiated icy mixtures of H_2O, H_2O_2 (with and without SO_2) in the 1–2.5 μm region will be needed to understand the role H_3O^+ and H_2O_2 play in affecting band shapes especially in the presence of different counter anions.

Another major result of this laboratory work is that we have confirmed the low temperature sequence $H_2S \rightarrow SO_2 \rightarrow$ ions + H_2SO_4 demonstrating that radiation-formed isolated ions (stable from 86–150 K) become structurally organized with warming to ~175 K, forming various crystalline hydrates mixed with crystalline water ice. With continued warming above 175 K, dehydration results in the loss of water. Although no high temperature (175 K or above) regions have been observed on Europa that would rapidly produce crystalline hydrate formation (Spencer et al., 1999), it is possible that radiation-induced ions will crystallize at diurnal temperatures over long time scales. Our results support the idea that sulfuric acid hydrates, made in non-crystalline mixtures of H_2SO_4 and H_2O, can co-exist at different temperatures in irradiated ices relevant to Europa.

In addition, our results show that hydrates can undergo dehydration in a vacuum environment and evolve, forming a sequence of hydrates, each richer in H_2SO_4 than the last, as a function of temperature and time. Our identification of both the tetrahydrate ($H_2SO_4{\cdot}4H_2O$) and the monohydrate ($H_2SO_4{\cdot}H_2O$) during warming was consistent with these being stable over the greatest temperature-concentration regions of the phase diagram for the SO_3–H_2O system (Gabel et al., 1950). Transient heating events on Europa may increase local surface temperatures sufficiently to dehydrate the surface and form these lower hydrates. However, it is the octahydrate ($H_2SO_4{\cdot}8H_2O$) and hemihexahydrate ($H_2SO_4{\cdot}6.5H_2O$) that provide the best overall match for the near IR data of Europa (Carlson et al., 1999a, 1999b, 2005). The near IR spectrum of the tetrahydrate showed only weak 1.5- and 2-μm water bands compared to the higher hydrates and is therefore considered to be a less attractive candidate. It is possible that in our heating experiments the octahydrate and hemihexahydrate formation preceded the tetrahydrate formation, but laboratory identification will require detailed hydrate data as a function of temperature. Reconciling both the mid- and near-IR spectra of these hydrates and changes in their spectra with removal or rearrangement of hydrate molecules during radiolysis will be a future study.

The distribution of hydrates on Europa correlates with the concentration of SO_2, the dark terrains, and impacting sulfur and oxygen plasma originating from Io (Carlson et al., 2005). Continuous radiolytic cycling of sulfur in its various forms results in a dynamic equilibrium with the relative abundances of sulfate, sulfur dioxide, and elemental sulfur established by production and loss mechanisms. In our experiments starting with H_2O/SO_2 ratios of 30, thought to be most applicable to Europa, we find that the SO_2 concentration attains a level of ~0.035 relative to the initial value (Fig. 10 and caption). We attribute this plateau level to equal production and destruction of SO_2, with most of the sulfur existing as SO_4^{2-} and other ions, and only 3.5% existing as SO_2. This relative concentration is consistent with observations. Hendrix and Carlson (in preparation) found SO_2 on Europa's trailing hemisphere with concentrations of 2.5×10^{17} molec cm^{-2} within the depth sampled by 200-to-300-nm ultraviolet measurements. Since Europa's reflectance is low in this spectral region, single scattering dominates and the depth that is probed will be comparable to the grain size. Using ice and acid grain diameters (54 and 12 μm, respectively) and a sulfate-to-H_2O ratio of 0.1 determined for Europa's trailing side (Carlson et al., 2005), we find Europa's SO_2 fraction to be 1.5 to 6.9%, consistent with the experimental value of 3.5%. These results indicate that SO_4^{2-} and other sulfur-containing ions are more stable under irradiation than is SO_2 and that these ionic components should be the major form in which sulfur exists on Europa.

Acknowledgments

The authors gratefully acknowledge Dr. Paul Wooldridge, a co-author of Zhang et al. (1993), who provided digital files of several H_2SO_4 hydrates. The authors also acknowledge support through The Goddard Center for Astrobiology, and NASA's Laboratory for Planetary Atmospheres and Planetary Geology and Geophysics programs. In addition, we thank Steve Brown, Claude Smith, and Eugene Gerashchenko, members of the Radiation Laboratory at NASA Goddard, for operation of the accelerator. R.L.H. acknowledges support from NASA Grant NNG05-GJ46G.

References

Calvin, W.M., Clark, R.N., Brown, R.H., Spencer, J.R., 1995. Spectra of the icy Galilean satellites from 0.2 to 5 μm: A compilation, new observations, and a recent summary. J. Geophys. Res. 100, 19041–19048.

Carlo, S.R., Grassian, V.H., 2000. Temperature-programmed desorption and reflectance absorption infrared spectroscopy of H_2O:HBr thin films of varying stoichiometry from 1:1 to 5:1. J. Phys. Chem. 104, 86–92.

Carlson, R.W., Anderson, M.S., Johnson, R.E., Smythe, W.D., Hendrix, A.R., Barth, C.A., Soderblom, L.A., Hansen, G.B., McCord, T.B., Dalton, J.B., Clark, R.N., Shirley, J.H., Ocampo, A.C., Matson, D.L., 1999a. Hydrogen peroxide on the surface of Europa. Science 283, 2062–2064.

Carlson, R.W., Johnson, R.E., Anderson, M.S., 1999b. Sulfuric acid on Europa and the radiolytic sulfur cycle. Science 286, 97–99.

Carlson, R.W., Anderson, M.S., Johnson, R.E., Schulman, M.B., Yavrouian, A.H., 2002. Sulfuric acid production on Europa: The radiolysis of sulfur in water ice. Icarus 157, 456–463.

Carlson, R.W., Anderson, M.S., Mehlman, R., Johnson, R.E., 2005. Distribution of hydrate on Europa: Further evidence for sulfuric acid hydrate. Icarus 177, 461–471.

Chandler, A.S., Choularton, T.W., Dollard, G.J., Eggleton, A.E.J., Gay, M.J., Hill, T.A., Jones, B.M.R., Tyler, B.J., Bandy, B.J., Penkett, S.A., 1988. Measurements of H_2O_2 and SO_2 in clouds and estimates of their reaction rate. Nature 338, 562–565.

Clark, R.N., 2004. The surface composition of Europa: Mixed water, hydronium, and hydrogen peroxide ice. In: Workshop on Europa's Icy Shell: Past, Present, and Future. Lunar and Planetary Institute, Houston, p. 16.

Clegg, S.M., Abbatt, J.P.D., 2001. Oxidation of SO_2 by H_2O_2 on ice surfaces at 228 K: A sink for SO_2 in ice clouds. Atmos. Chem. Phys. Discuss. 1, 77–92.

Cooper, J.F., Johnson, R.E., Mauk, B.H., Garrett, H.B., Gehrels, N., 2001. Energetic ion and electron irradiation of the icy Galilean satellites. Icarus 149, 133–159.

Couling, S.B., Nash, K.L., Fletcher, J., Henderson, A., Vickerman, J.C., Horn, A.B., 2003. Identification of surface molecular hydrates on solid sulfuric acid films. J. Am. Chem. Soc. 125, 13038–13039.

Ferraro, J.R., Sill, G., Fink, U., 1980. Infrared intensity measurements of cryodeposited thin films of NH_3, NH_4HS, H_2S, and assignments of absorption bands. Appl. Spectrosc. 34, 525–533.

Fink, U., Sill, G.T., 1982. The infrared spectral properties of frozen volatiles. In: Wilkening, L. (Ed.), Comets. Univ. of Arizona Press, Tucson, pp. 164–202.

Gable, C.M., Betz, H.F., Maron, S.H., 1950. Phase equilibria of the system sulfur trioxide–water. J. Am. Chem. Soc. 72, 1445–1448.

Gomis, O., Leto, G., Strazzulla, G., 2004a. Hydrogen peroxide production by ion irradiation of thin water ice films. Astron. Astrophys. 420, 405–410.

Gomis, O., Satorre, M.A., Strazzulla, G., Leto, G., 2004b. Hydrogen peroxide formation by ion implantation in water ice and its relevance to the Galilean satellites. Planet. Space Sci. 52, 371–378.

Grundy, W.M., Buie, M.W., Stansbury, J.A., Spencer, J.R., Schmitt, B., 1999. Near-infrared spectra of icy outer Solar System surfaces: Remote determination of H_2O ice temperatures. Icarus 142, 536–549.

Hall, D.T., Feldman, P.D., McGrath, M.A., Strobel, D.F., 1998. The far-ultraviolet oxygen airglow of Europa and Ganymede. Astrophys. J. 499, 475–481.

Hall, D.T., Strobel, D.F., Feldman, P.D., McGrath, M.A., Weaver, H.A., 1995. Detection of an oxygen atmosphere on Jupiter's moon Europa. Nature 373, 677–679.

Horn, A.B., Sully, K.J., 1999. ATR-IR spectroscopic studies of the formation of sulfuric acid monohydrate films. Phys. Chem. Chem. Phys. 1, 3801–3806.

Hudson, R.L., Moore, M.H., 2004. Reactions of nitriles in ices relevant to Titan, comets, and the interstellar medium: Formation of cyanate ion, ketenimines, and isonitriles. Icarus 172, 466–478.

Isoniemi, E., Khriachtchev, L., Pettersson, M., Räsänen, M., 1999. Infrared spectroscopy and 266 nm photolysis of H_2S_2 in solid Ar. Chem. Phys. Lett. 311, 47–54.

Johnson, R.E., Nelson, M.L., McCord, T.B., Gradie, J.D., 1988. Analysis of Voyager images of Europa—Plasma bombardment. Icarus 75, 423–436.

Johnson, R.E., Killen, R.M., Waite Jr., J.H., Lewis, W.S., 1998. Europa's surface composition and sputter-produced ionosphere. Geophys. Res. Lett. 17, 3257–3260.

Johnson, R.E., Quickenden, T.I., Cooper, P.D., McKinley, A.J., Freeman, C.G., 2003. The production of oxidants in Europa's surface. Astrobiology 3, 823–850.

Johnson, R.E., Cooper, P.D., Quickenden, T.I., Grieves, G.A., Orlando, T.M., 2005. Production of oxygen by electronically induced dissociations in ice. J. Chem. Phys. 123, 184715–184722.

Kargel, J.S., Kaye, J., Head, J.W.I., Marion, G., Sassen, R., Crowley, J., Prieto, O., Hogenboom, D., 2000. Europa's crust and ocean: Origin, composition, and prospects for life. Icarus 94, 368–390.

Kargel, J.S., Head III, J.W., Hogenboom, D.L., Khurana, K.K., Marion, G., 2001. The system sulfuric acid–magnesium sulfate–water: Europa's ocean properties related to thermal state. Lunar Planet. Sci. XXXII. Abtract 2138.

Lane, A.L., Nelson, R.M., Matson, D.L., 1981. Evidence for sulfur implantation in Europa's UV absorption band. Nature 292, 38–39.

Larson, L.J., Kuno, M., Tao, F., 2000. Hydrolysis of sulfur trioxide to form sulfuric acid in small water clusters. J. Chem. Phys. 112, 8830–8838.

Loeffler, M.J., Baragiola, R.A., 2005. The state of hydrogen peroxide on Europa. Geophys. Res. Lett. 32, 17202–17204.

Loeffler, M.J., Raut, U., Vidal, R.A., Baragiola, R.A., Carlson, R.W., 2006. Synthesis of hydrogen peroxide in water ice by ion irradiation. Icarus 180, 265–273.

Liuti, G., Dondes, S., Harteck, P., 1966. The reaction of hydrogen sulfide and atomic oxygen. J. Am. Chem. Soc. 88, 3212–3215.

Marion, G., 2002. A molal-based model for strong acid chemistry at low temperatures (187 to 298 K). Geochim. Cosmochim. Acta 66, 2499–2516.

McCord, T.B., Hansen, G.B., Clark, R.N., Martin, P.D., Hibbits, C.A., Fanale, F.P., Granahan, J.C., Segura, M., Matson, D.L., Johnson, T.V., Carlson, R.W., Smythe, W.D., Danielson, G.E., the NIMS team, 1998a. Non-water-ice constituents in the surface material of the icy Galilean satellites from the Galileo near-infrared mapping spectrometer investigation. J. Geophys. Res. 103, 8603–8626.

McCord, T.B., Hansen, G.B., Fanale, F.P., Carlson, R.W., Matson, D.L., Johnson, T.V., Smythe, W.D., Crowley, J.L., Martin, P.D., Ocampo, A., Hibbitts, C.A., Granahan, J.C., 1998b. Salts on Europa's surface detected by Galileo's near infrared mapping spectrometer. Science 280, 1242–1245.

McCord, T.B., Hansen, G.B., Matson, D.L., Johnson, T.V., Crowley, J.K., Fanale, F.P., Carlson, R.W., Smythe, W.D., Martin, P.D., Hibbitts, C.A., Granahan, J.C., Ocampo, A., 1999. Hydrated salt minerals on Europa's surface from the Galileo NIMS investigation. J. Geophys. Res. 104, 11827–11852.

McCord, T.B., Orlando, T.M., Teeter, G., Hansen, G.B., Sieger, M.T., Petrik, N.K., Van Keulen, L., 2001. Thermal and radiation stability of the hydrated minerals epsomite, mirabilite, and natron under Europa environmental conditions. J. Geophys. Res. 106, 311–331.

McCord, T.B., Teeter, G., Hansen, G.B., Sieger, M.T., Orlando, T.M., 2002. Brines exposed to Europa surface conditions. J. Geophys. Res. 107, 4-1–4-6.

McEwen, A.S., 1986. Exogenic and endogenic albedo and color patterns on Europa. Geophys. Res. 91, 8077–8097.

Moore, M.H., 1984. Infrared studies of proton irradiated SO_2 ices: Implications for Io. Icarus 59, 114–128.

Moore, M.H., Hudson, R.L., 2000. IR detection of H_2O_2 at 80 K in ion-irradiated laboratory ices relevant to Europa. Icarus 145, 282–288.

Moore, M.H., Hudson, R.L., 2003. Infrared study of ion irradiated N_2-dominated ices relevant to Triton and Pluto: Formation of HCN and HNC. Icarus 161, 486–500.

Nash, K.L., Sully, K.J., Horn, A.B., 2000. Infrared spectroscopic studies of the low temperature interconversion of sulfuric acid hydrates. Phys. Chem. Chem. Phys. 2, 4933–4940.

Noll, K.S., Weaver, H.A., Gonnella, A.M., 1995. The albedo spectrum of Europa from 2200 angstrom to 3300 angstrom. J. Geophys. Res. 100, 19057–19059.

Noll, K.S., Johnson, R.E., Lane, A.L., Domingue, D.L., Weaver, H.A., 1996. Detection of ozone on Ganymede. Science 273, 341.

O'Shaughnessy, D.J., Boring, J.W., Johnson, R.E., 1988. Measurements of reflectance spectra of ion-bombarded ice and application to surfaces in the outer Solar System. Nature 333, 240–241.

Palmer, K.F., Williams, D., 1975. Optical constants of sulfuric acid. Application to the clouds of Venus? Appl. Opt. 14, 208–219.

Pichler, A., Fleissner, G., Hallbrucker, A., Mayer, E., 1997. FT-IR spectroscopic monitoring of alkali metal disulfite and hydrogensulfite in freeze-concentrated and glassy aqueous solution. Implications for atmosphere chemistry. J. Mol. Struct. 408, 521–525.

Pierazzo, E., Chyba, C.F., 2002. Cometary delivery of biogenic elements to Europa. Icarus 157, 120–127.

Querry, M.R., Waring, R.C., Holland, W.E., Earls, L.M., Herrman, M.D., Nijm, W.P., Hale, G.M., 1974. Optical constants in the infrared for K_2SO_4, $NH_4H_2PO_4$, and H_2SO_4 in water. J. Opt. Soc. Am. 64, 39–46.

Salama, F., Allamandola, L.J., Witteborn, F.C., Cruikshank, D.P., Sandfore, S.A., Bregman, J.D., 1990. The 2.5–5.0 μm spectra of Io: Evidence for H_2S and H_2O frozen in SO_2. Icarus 83, 66–82.

Schriver-Mazzuoli, L., Chaabouni, H., Schriver, A., 2003a. Infrared spectra of SO_2 and SO_2:H_2O ices at low temperature. J. Mol. Struct. 644, 151–164.

Schriver-Mazzuoli, L., Schriver, A., Chaabouni, H., 2003b. Photo-oxidation of SO_2 and of SO_2 trapped in amorphous water ice studied by IR spectroscopy. Implications for Jupiter's satellite Europa. Can. J. Phys. 81, 301–309.

Smythe, W.D., Carlson, R.W., Ocampo, A., Matson, D., Johnson, T.V., McCord, T.B., Hansen, G.E., Soderblom, L.A., Clark, R.N., 1998. Absorption bands in the spectrum of Europa detected by the Galileo NIMS instrument. Lunar Planet. Sci. XXIX. Abstract 1532.

Spencer, J.R., Calvin, W.M., 2002. Condensed O_2 on Europa and Callisto. Astron. J. 24, 3400–3403.

Spencer, J.R., Klesman, A., 2001. New observations of molecular oxygen on Europa and Ganymede (abstract). Bull. Am. Astron. Soc. 33, 1125.

Spencer, J.R., Calvin, W.M., Person, M.J., 1995. Charge-coupled-device spectra of the Galilean satellites: Molecular-oxygen on Ganymede. Geophys. Res. 100, 19049–19056.

Spencer, J.R., Tampari, L.K., Martin, T.Z., Travis, L.D., 1999. Temperatures on Europa from Galileo photopolarimeter–radiometer: Nighttime thermal anomalies. Science 284, 1514–1516.

Strazzulla, G., Leto, G., Palumbo, M.E., 1993. Ion irradiation experiments. Adv. Space Res. 13, 189–198.

Teolis, B.D., Loeffler, M.J., Raut, U., Famá, M., Baragioloa, R.A., 2006. Ozone synthesis on the icy satellites. Astron. J. 644, L141–L144.

Tso, T., Lee, E.K.C., 1984. Formation of sulfuric acid and sulfur trioxide/water complex from photooxidation of hydrogen sulfide in solid O_2 at 15 K. J. Phys. Chem. 88, 2776–2881.

Zhang, Z., Ewing, G.E., 2002. Infrared spectroscopy of SO_2 aqueous solutions. Spectrochim. Acta 58, 2105–2113.

Zhang, Z., Ewing, G.E., 2004. Infrared studies of the SO_2 clathrate hydrate. J. Phys. Chem. A 108, 1681–1686.

Zhang, R., Wooldridge, P.J., Abbatt, J.P.D., Molina, M.J., 1993. Physical chemistry of the H_2SO_4/H_2O binary system at low temperatures: Stratospheric implications. J. Phys. Chem. 97, 7351–7358.

Ziegler, J.P., Biersack, J.P., Littmark, U., 1985. The Stopping and Range of Ions in Solids. Pergamon, New York. See also http://www.srim.org.